Extreme warming of Amazon waters in a changing climate

Ayan Fleischmann[1]*, Fabrice Papa[2,3], Stephen Hamilton[4], John Melack[5], Bruce Forsberg[6], Adalberto Val[7], Walter Collischonn[8], Leonardo Laipelt[8], Júlia Brusso Rossi[8], Bruno Comini de Andrade[8], Bruna Mendel[1], Priscila Alves[1], Maiby Bandeira[9,10], Lady Custódio[1], Maria Cecília Gomes[1], Débora Hymans[1], Isabela Keppe[1], Raize Mendes[9,10], Renan Nascimento[9,10], Paula dos Santos Silva[1], Camila Vieira[1], Rodrigo Xavier[1], André Zumak[1], Anderson Ruhoff[8], Wencai Zhou[5], Sally MacIntyre[5], Eduardo G. Martins[11], Naziano Filizola[12], Rogério Marinho[12], Ednaldo Bras Severo[12], Mariana Frias[13], Renata Oliveira[14], Lucas Lauretto[14], Waleska Gravena[15], André Coelho[1], Hilda Chávez-Pérez[1], Susana Braz-Mota[7], Michel Nasser[16], Daniel Medeiros Moreira[17], Leandro Guedes Santos[18], José Reinaldo Pacheco Peleja[19], Miriam Marmontel[1]

[1]Instituto de Desenvolvimento Sustentável Mamirauá, Tefé, Brazil
[2]Laboratoire d'Etudes en Géophysique et Océanographie Spatiales (LEGOS), Université Toulouse, IRD, CNRS, CNES, UPS, Toulouse, France
[3]Institut de Recherche pour le Développement (IRD), Institute of Geosciences, Campus Universitário Darcy Ribeiro, Universidade de Brasília (UnB), Brasília, Brazil
[4]Kellogg Biological Station, Michigan State University, Hickory Corners, Michigan, and Cary institute of Ecosystem Studies, Millbrook, New York, USA
[5]Earth Research Institute, University of California, Santa Barbara, CA, USA
[6]Brazilian National Institute for Research of the Amazon, LBA program, Manaus, Brazil
[7]INPA - Brazilian National Institute for Research of the Amazon, Laboratory of Ecophysiology and Molecular Evolution (LEEM), Manaus, Brazil
[8]Hydraulic Research Institute (IPH), Federal University of Rio Grande do Sul (UFRGS), Porto Alegre, Brazil
[9]INPA - Brazilian National Institute for Research of the Amazon, Laboratory of Plankton, Manaus, Brazil
[10]Aqua Viridi, Manaus, Brazil
[11]University of Northern British Columbia, Prince George, Canada
[12]Grupo de Pesquisa H2A, Federal University of Amazonas (UFAM), Manaus, Brasil
[13]WWF-Brasil, Brasília, Brazil
[14]ICMBio NGI Tefé, Tefé, Brazil
[15]Instituto de Saúde e Biotecnologia, Universidade Federal do Amazonas (UFAM), Coari, Brazil
[16]Universidade Federal do Amazonas (UFAM), Coari, Brazil
[17]Geological Survey of Brazil, Rio de Janeiro, Brazil
[18]Geological Survey of Brazil, Belém, Brazil
[19]Federal University of Western Pará, Santarém, Brazil

*Corresponding author. Email: ayan.fleischmann@mamiraua.org.br

The paper is a non-peer reviewed preprint submitted to EarthArXiv. The preprint was submitted to *Science* for peer review.

Abstract: In 2023, an unprecedented drought and heatwave severely impacted Amazon waters, leading to high mortality of fishes and river dolphins. Five of 10 lakes monitored showed exceptionally high daytime temperatures (>37°C), with one large lake reaching up to 41°C in the entire ~2-m deep water column, with up to 13°C of diel variation. Modeling show that high solar radiation, reduced water depth and wind speed, and turbid waters are the main drivers of the high temperatures. This extreme heating of Amazon waters follows a long-term increase of 0.6°C/decade revealed by satellite estimates across the region's lakes between 1990 and 2023. With ongoing climate change, temperatures that approach or exceed thermal tolerances for aquatic life are likely to become more common in tropical aquatic systems.

Main Text:

The temperature of aquatic ecosystems is a fundamental variable that influences biogeochemical and ecological processes and directly and indirectly affects aquatic life. In recent decades, many lakes have warmed, averaging 0.34°C/decade globally (*1*), and maximum near-surface temperatures of large lakes in Europe have warmed up to 0.58 °C/decade on average (*2*). This increase is projected to continue under ongoing climate change, coinciding with more frequent severe lake heatwaves (*3*, *4*). Indeed, lakes are considered sentinels of climate change (*5*), but most studies of warming lakes are from temperate to subtropical regions. This overlooks potential impacts of climate change on tropical systems, where diel patterns in thermal stratification and mixing as well as dissolved oxygen are often more pronounced than in higher latitudes (*6*, *7*). In shallow waters, diel variations in surface energy fluxes lead to strong vertical thermal gradients during daytime heating, followed by vertical mixing during overnight cooling (*8–10*). Amazon floodplain lakes also have large seasonal changes in water levels and in optical properties, both of which strongly influence stratification and mixing patterns (*11*).

The year 2023 experienced major heatwaves across the globe with record-breaking air temperatures and a prolonged heatwave in the Amazon region (*12*). Furthermore, in September and October 2023, a record-breaking drought occurred in the Amazon, with the lowest river water levels ever recorded (*13*). The unprecedented drought intensity has been attributed to climate change, including widespread warming of the oceans, in particular of the North Atlantic, in combination with a moderate-to-strong El Niño event[13-15].

While heatwaves during 2023 were reported for air and marine temperatures around the globe (*14*, *15*), here we reveal extreme heating of tropical inland waters of the Amazon. We present water temperature measurements during the 2023 drought for 10 Amazonian lakes and provide a regional-scale perspective based on satellite observations of water temperatures. Hydrodynamic simulations further reveal the drivers of lake warming. As a consequence of this extreme drought-heatwave event, thousands of people living in riparian communities were isolated without proper access to food, potable water and medicine. An unprecedented massive mortality of Amazon river and tucuxi dolphins occurred, likely associated with extreme water temperatures (*16*, *17*). The measured temperatures, up to 41.0°C in the shallow waters of Tefé Lake (0.5 to 2 m), are in the upper range of measurements reported in tropical inland waters. These observations highlight the major threats that will likely affect the people and biodiversity of the Amazon and other tropical waters in years to come.

Extreme heating of Tefé Lake

Tefé Lake became the focus of national and international attention during the 2023 Amazon drought (Fig. 1) because of massive, unprecedented mortality of freshwater dolphins (*Inia geoffrensis* and *Sotalia fluviatilis*) between late Sep and Oct 2023, leading to 209 carcasses found in a short interval (*17*). Between Sep 24 and Oct 26, the lake's surface area decreased by 75% from 379 to 95 km² (see satellite images in Fig. 1a), with large portions of the lake less than 0.5 m deep over an 8-km reach (Fig. 1b). Spatial and temporal measurements of water temperatures were made beginning on Oct 1 (Fig. 1a; Methods).

Tefé Lake is a ria lake (also known as blocked fluvial valley (*18*)), a common geomorphology in the central Amazon formed by backflooding of tributaries close to their confluences with the Amazon River (*19*). Tefé Lake is around 60 km long and is normally more than 7 km wide close to the city of Tefé. Our measurements detected a maximum water temperature of 41.0°C on Oct 18 (at site 2; Fig. 1b), and a high diel variation of up to 13.3°C (from 41.0°C on Oct 18 15h30 local time to 27.7°C on Oct 19 at 7h00), associated with intense nocturnal cooling. Afternoon temperatures reached more than 37°C in parts of Tefé Lake on 19 days in October (Fig. 1c). Along the 9-km channel that drains the lake into the Amazon River, temperatures decreased from the lake to the confluence (Fig. 1c). A survey on Oct 2 found a change from 37.4°C in the upstream part of the channel to 31.3°C in the Amazon River (Fig. S1), and temperatures decreased from 40°C to 36°C in a distance of less than 3 km on Oct 18 (Fig. 1c).

To examine environmental drivers of the extreme temperatures, we performed a set of numerical simulations with a well-calibrated hydrodynamic model developed at a similar Amazonian lake (Fig. 2; Supplementary Text; Zhou et al. (*11*)) – lack of enough in situ data precludes the development of such a model for Tefé Lake. When simulating conditions similar to those observed in the 2023 heatwave, the modelled temperatures reached up to 42°C due to a combination of factors, including shallow and turbid water, clear skies with high sunlight, low wind speed, and slightly elevated air temperature. All these factors occurred in Lake Tefé in the 2023 drought: reduced water depth (less than 0.5 m along more than eight km of the lake), high solar radiation (a sequence of 11 days without clouds, Fig. S2 and Fig. S3), and very turbid waters (Secchi disk depth less than 0.15 m; Fig. S4). Consequently, afternoon peak water temperatures in Tefé Lake increased each day over the consecutive clear-sky days as the lake gained heat (Fig. S5).

High air temperatures were recorded at weather stations across the central Amazon, breaking records, including at Tefé (maximum surface air temperature in Tefé was 39.1°C on Sep 28; Fig. S6). However, significant heat was not gained by sensible heat exchange (Fig. 2 and Supplementary Text). Advection of heat from the lake to its outlet channel led to extreme temperatures along the channel (where most of the dolphins died). Water temperatures gradually decreased due to heat dissipation as water flowed along the 9-km channel at velocities up to 0.7 m s^{-1} and discharge of ~50 m^3 s^{-1} (Fig. 1e) toward the channel's confluence with the Amazon River (Fig. 1c and Fig. S1).

From mid-November onward, continuous water level and temperature measurements (site 4; Fig. 1b) enabled monitoring of the lake's return to more normal water temperatures. As the depth increased, diurnal thermal stratification of the water column occurred (Fig. S5). After water

levels increased more than 1.5 m (by Nov 21) above the minimum water level (reached on Oct 23), the diel variation of water temperature was reduced, with a maximum observed range of 29.5–34.5°C at 0.3 m and 29.5–31.7°C at 2 m after Dec 20.

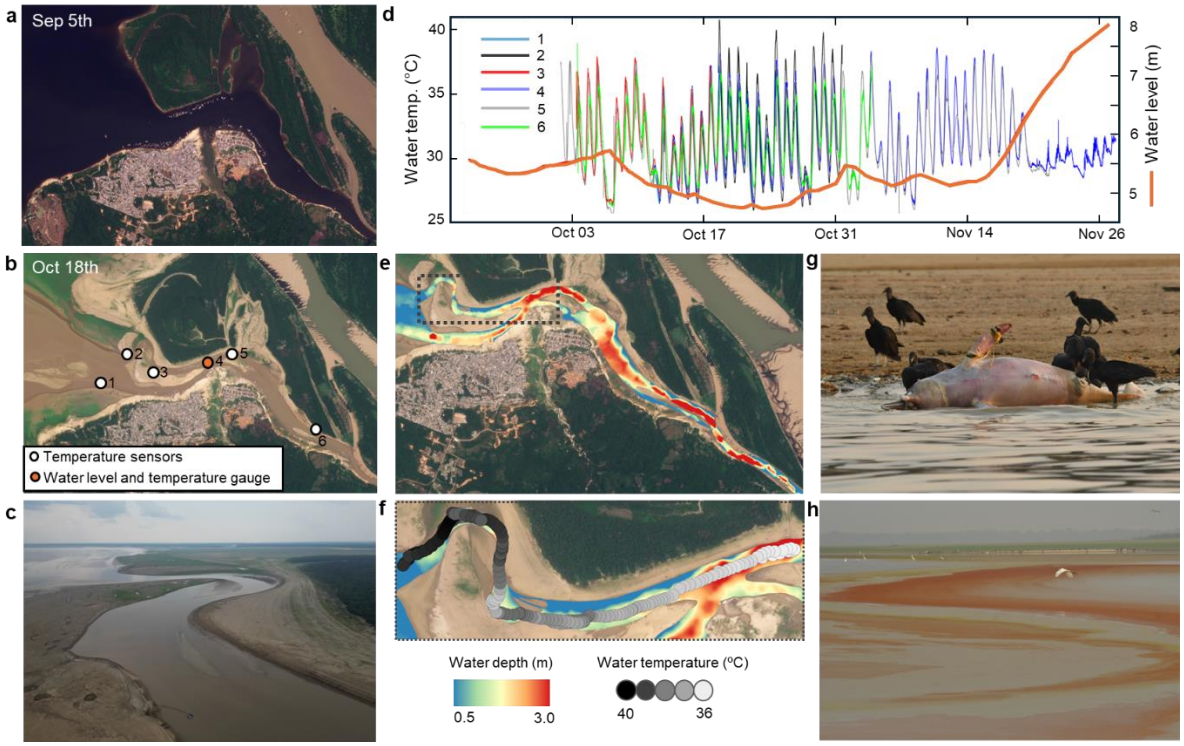

Fig. 1. Major drought and heating of Tefé Lake waters in 2023, reaching more than 40°C in the whole water column. (a) Changes in lake surface area from early Sep to **(b)** Oct 2023 in Tefé Lake, based on Planet satellite imagery. **(c)** Aerial photograph of the lake in October. **(d)** Water temperatures and level changes (location of sensors in panel b) in Tefé Lake during the 2023 drought show the extreme values. **(e)** Lake bathymetry and **(f)** profile of surface water temperatures for a survey on Oct 18 reveal the longitudinal gradient of temperature along the channel. **(g)** Photos of the drought in Tefé Lake show a dead Amazon River dolphin and **(h)** a surface scum of the phytoplanktonic *Euglena sanguinea*.

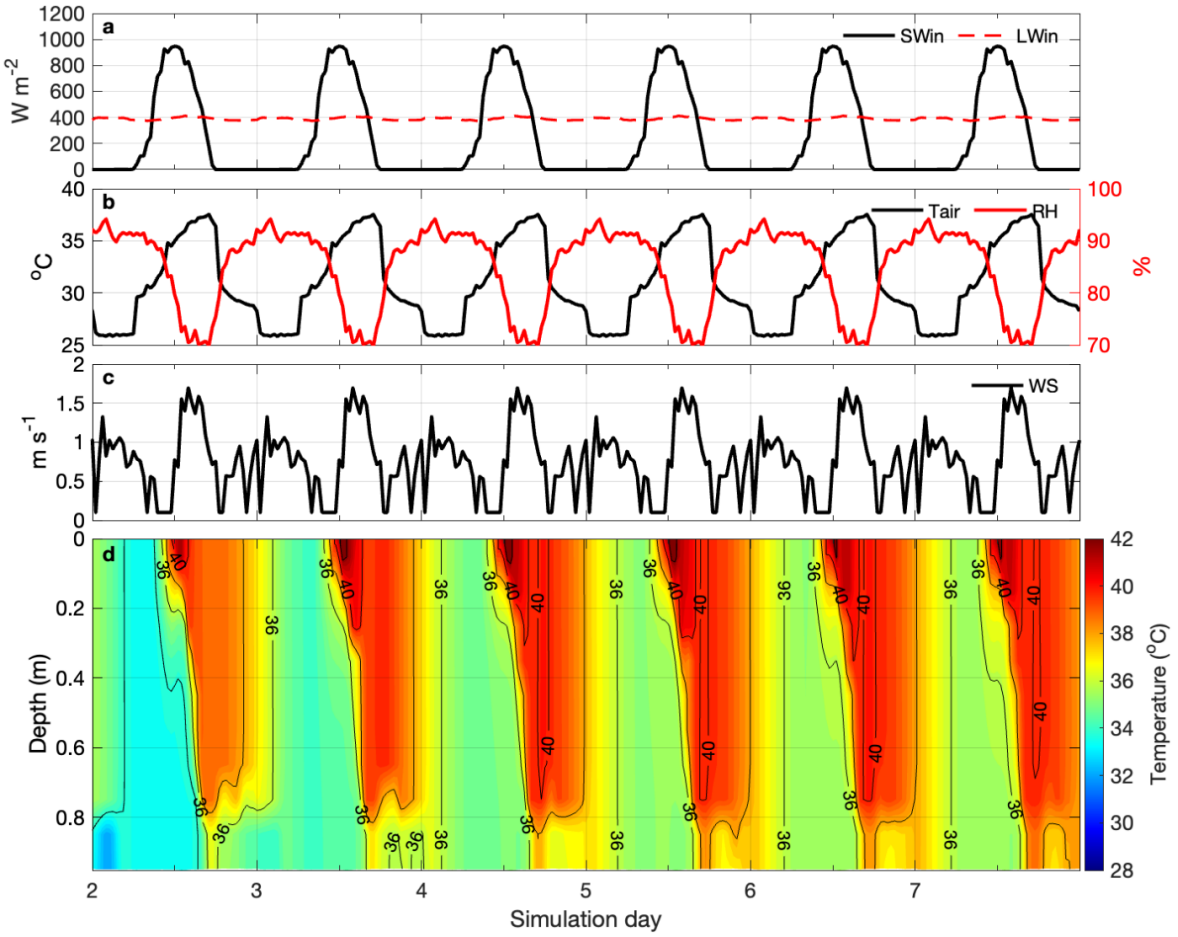

Fig. 2. Numerical simulations enlighten the drivers of large heating of an Amazonian lake during drought conditions. (a) Incoming shortwave radiation (SWin) and longwave radiation (LWin); **(b)** air temperature (Tair) 20% higher than measured values (black), and measured relative humidity (RH); **(c)** wind speed (WS) reduced to 30%; **(d)** simulated temperatures, with surface water values exceeding 40°C around noon within three days of starting the simulation.

Heating of Amazonian lakes in 2023 was widespread

Water temperatures measured *in situ* during the drought in 10 central Amazon lakes, as well as in a reach of the lower Amazon River (Fig. 3a and Fig. S7), revealed high values in most cases, with temperatures above 37°C measured in five lakes. In Coari Lake, which is similar to Tefé Lake in size and geomorphology, water temperatures exhibited high diel variation (Fig. S8). The maximum temperature was 37.5°C, but measurements (Nov 3-28) were made after the heatwave peak so temperatures had likely reached higher values in the preceding weeks. Surveys of water depth during the drought found shallow waters (less than 0.5 m) over extensive areas. Coari Lake's larger watershed area and higher outflow discharge could explain the less extreme water temperatures in comparison to Tefé Lake.

For the other lakes sampled in Nov 2023, high water temperatures were also observed, though measurements started after the peak heatwave in October. A few ria lakes, such as Amanã Lake (Fig. 3a), remained deeper and cooler during the drought. In comparison to Tefé and Coari lakes, continuous water temperature measurements available for two other smaller floodplain lakes in the vicinity showed lower average water temperatures and diel ranges (Fig. 1d and 3b), although diel ranges increased markedly during the heatwave. These lakes were disconnected from the main river during the drought and had water depths over 1 m.

Water temperatures measured in the lower Amazon River in 2021 and 2023 provide further evidence for the unusual heating of the river system in Sep-Nov 2023, with surface temperatures consistently higher than in 2021 (Fig. S7). In the lower Negro River, in the Anavilhanas archipelago, surface water temperature higher than 37°C was also measured (N. Filizola, *pers. comm.*) – in this area, backflooding by the Amazon River waters causes a reduction in flow velocity.

Our findings are remarkable in three aspects. First, temperatures approaching or higher than 40°C in large waterbodies are rare even for tropical systems. This is much higher than the systems' usual temperatures: average surface water temperature in tropical lakes are typically around 29–30°C (*20*); for instance, an average of 30.4°C was obtained for a total of 322 samples obtained in 24 different Amazon floodplain lakes between 1995 and 2011 (data from SO Hybam network; available at: <https://hybam.obs-mip.fr/documents/field-campaign-reports/brazil/>). Monthly measurements in Tefé Lake from 2004 to 2020 showed a maximum near-surface temperature of 33.3°C in 2012 (long-term average of 29.1°C). In Amazonian forest streams, temperatures usually range between 25 and 28°C (*21*), whereas a maximum value of 31°C has been reported for the Negro River, a major tributary of the Amazon River (*22*). The 2023 observations in Tefé Lake exceeded maximum water temperatures recorded in Lake Curuai, a floodplain lake in the lower Amazon, during low water (36.6°C in 2005; temperatures above 35°C were also observed in 2004 and 2010). Water temperatures in shallow, vegetated waters of the Pantanal wetland in Brazil rarely exceeded 35°C over the course of a year (*6*). Temperatures in a slowly flowing, unshaded tropical river in northern Australia ranged from 28–38°C over 24 hours (*6*).

Second, although near-surface temperature can sometimes reach values as high as 40°C during diurnal stratification in tropical lakes, temperatures usually decrease with depth, but they remained high throughout the shallow water column of Tefé Lake. Measurements over two years at a series of depths in open water in Janauacá Lake on the central Amazon floodplain ranged from 27.5–35.5°C, but reached 40°C in near-surface waters within floating plant stands (Zhou et al. (*11*); J. Melack and S. MacIntyre, unpublished data). In Cedrinho Lake on the floodplain of the Purus River (a tributary of the Amazon River), near-surface water temperature reached 41°C in December 2016, but decreased to around 30°C (max. 32.6°C) at a depth of 0.3 m (E. Martins, unpublished data). In contrast, during the 2023 drought, in the shallow water of Tefé Lake (up to 2 m deep in some locations) when temperatures as high as 40°C were being measured, no cooler water was present at depth to provide a refuge from high temperatures.

Third, the high diel temperature range in Tefé and Coari lakes are at the upper limit of the values reported by a recent synthesis of 100 lakes, although none were in the tropics (*23*). The highest average diel amplitude reported was 7°C for small lakes, with a maximum value of around 15°C near surface in a very small temperate lake (Jekl Bog; surface area 2500 m²). In the much larger

Tefé Lake, we observed a 13.3°C diel range along the entire water column (as deep as 2 m at some points).

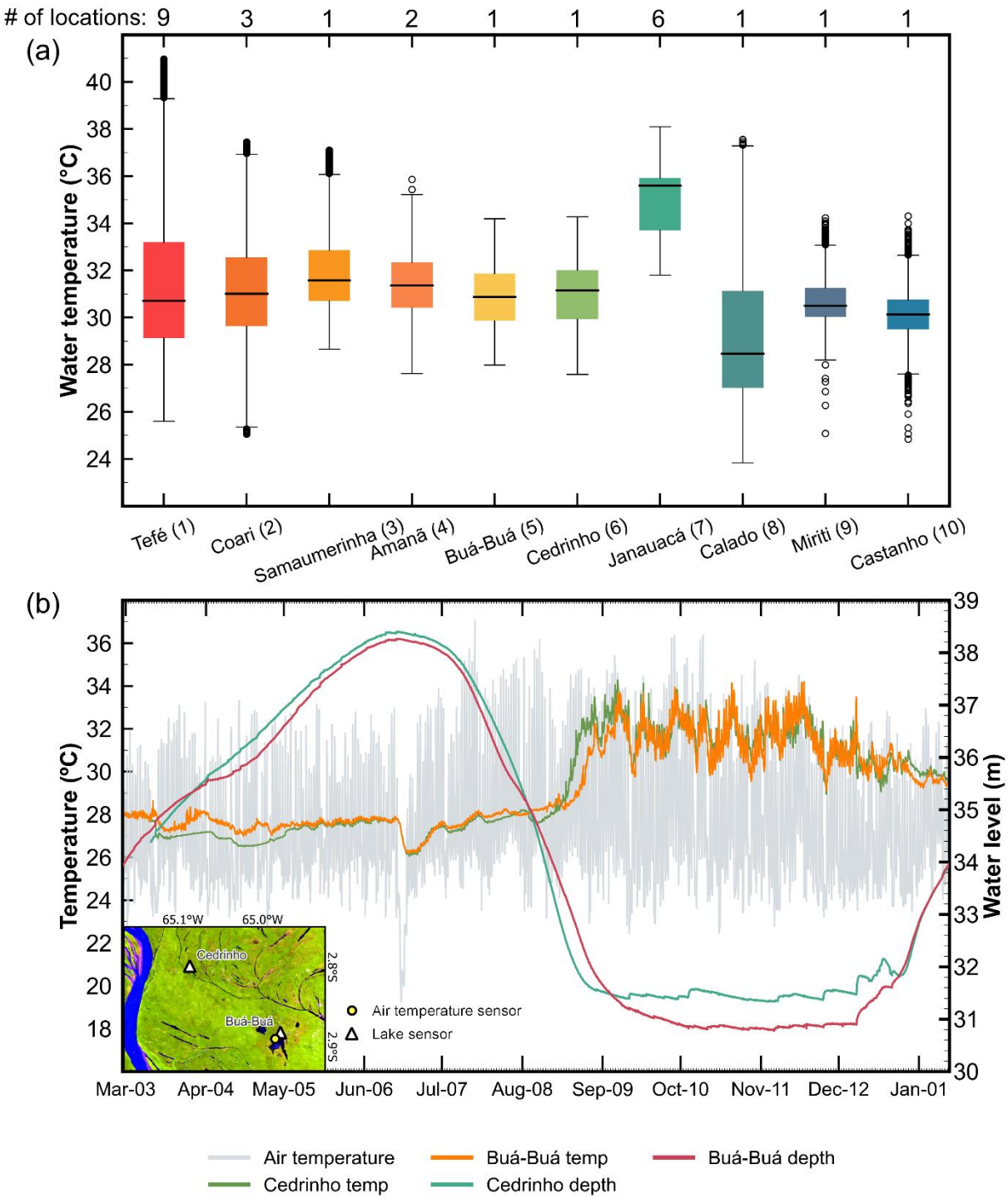

Fig. 3. Widespread heating in Central Amazon lakes. (a) *In situ* measurements show high water temperatures in 10 central Amazon lakes during the 2023 drought. The number of monitoring sites per lake is shown at the top, and the location of the lakes is presented in the map

of Figure 4. **(b)** Water levels, water temperature, and air temperature (hourly resolution) in two central Amazon floodplain lakes within the Mamirauá Sustainable Development Reserve near Tefé show increases in temperatures (both magnitude and diel variation) during the low water period when the heatwave occurred.

Long-term water temperature trends at the regional scale

In recent decades (1990-2023), the mean surface-water temperature in central Amazon water bodies has increased by 0.6°C/decade based on Landsat satellite observations of 24 large lakes (Fig. 4; see Methods and Fig. S9). All assessed lakes have significant positive trends ($P<0.05$), with Tefé and Coari lakes showing an increase of 0.7°C/decade, and maximum trends of 0.8°C/decade for Tapajós, Badajós and Amanã lakes (Fig. S9). Positive surface water temperature anomalies were more frequent over the last decade (2013-2023), with a sequence of positive anomalies observed since 2018 (Fig. 4b). Other studies have reported increasing water temperature trends for lakes across the globe (*24*), although the trends we report here are higher than those reported by O'Reilly et al.(*1*) The trends reported here may be higher because in the Amazon region cloud-free days for multispectral images occur mostly during the dry (warmer) season (72% of available images were from Jun-Oct).

Our remote sensing estimates of average surface water temperature across the 24 lakes clearly depict the high water temperatures in 2023 (Fig. 4a). During the 2023 heatwave, the surface water extent was reduced in the whole region, with some lakes falling to less than 10% of their usual open-water area (Fig. 4c). Tefé Lake was reduced in area by 75%, and the largest change was observed for Badajós Lake (92%). This large reduction in water surface extent occurred due to reduced river levels, and the shallow depths coincided with the exceptional heating of the water bodies. Remote sensing estimates provide further evidence that Tefé Lake water temperatures were higher than in most other large lakes in the central Amazon (red pixels in the detail of Fig. 4a).

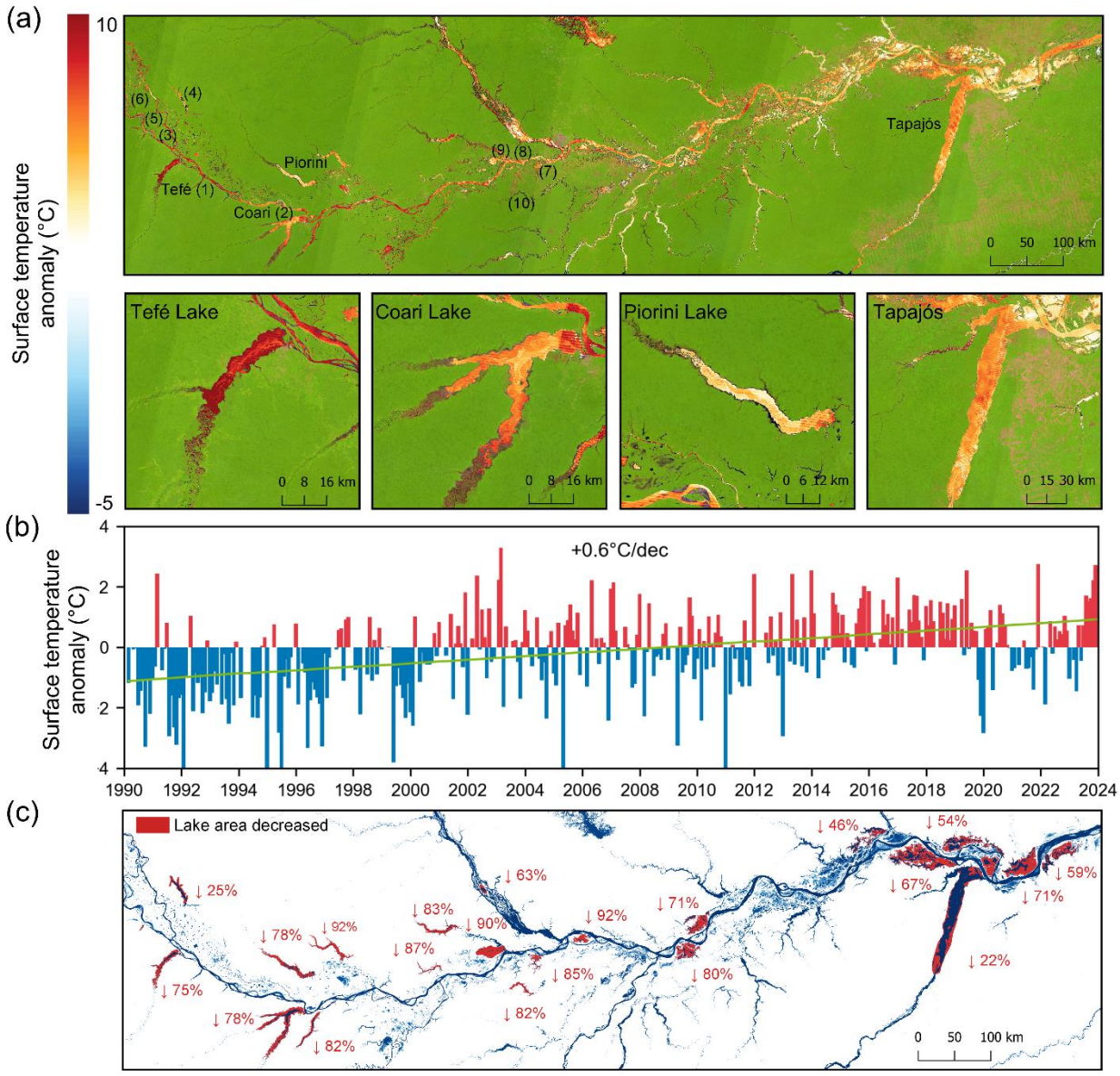

Fig. 4. (a) Long-term heating of Central Amazon lakes, and major warming in 2023. Landsat observations of water temperatures during the 2023 drought in the central Amazon show positive anomalies for many water bodies (Sep-Oct 2023 anomaly map in relation to the 1990-2023 Sep-Oct average), and details are shown for four lakes. The numbers in parentheses refer to the lakes with in situ data in Fig. 3. **(b)** Anomalies of long-term mean monthly temperature for 24 lakes in the central Amazon show a positive trend of 0.6°C/decade. (**c**) Decrease in lake surface water during the 2023 extreme drought.

Socio-ecological implications

While impacts of climate change on increasing water temperatures have been reported in detail for certain biomes, such as lakes at northern latitudes (*20*, *25*) and marine ecosystems including coral reefs (*26*), the ecological consequences of increasing water temperatures in tropical and

subtropical freshwaters have received much less attention. On the day 39.5°C was first measured in Tefé Lake (Sep 28), 70 carcasses (59 Amazon River dolphins and 11 tucuxi dolphins) were found in the lake; the whole mortality event, during less than two months, led 209 dolphins to die, an unprecedented observation in the Amazon, and a high percentage of the estimated dolphin population in Tefé Lake. The reasons why the dolphins stayed in the overheated water are unclear, since the lake's channel had a longitudinal decrease in water temperatures towards the Amazon River, which could have been accessed by the animals. Perhaps neurological effects of the high temperatures caused the animals to not move toward the cooler downstream waters (*27*). The mortality of these animals attracted national and international attention because they are charismatic, and the event was of an unusual nature, whereas the impacts of the heatwave on other freshwater fauna received much less attention.

The exceptionally low water level caused numerous problems for local human inhabitants who use the river and floodplain lakes for transportation and fishing. In particular, major fish mortality was also observed in some Amazonian reservoirs and lakes during the 2023 drought. Drainage of many large floodplain lakes connected to the river must have displaced fish populations into the major rivers, whose volume was also diminished, and the fate of those fish is unknown, though mortality likely ensued. Tropical ectotherms, like Amazon fishes, have narrow thermal tolerance ranges, so even relatively small increases in temperature can result in high mortality [34]. Among tropical species assessed in a laboratory setting, Amazonian fishes seem particularly sensitive to warm temperature[37], and declines in survival have been observed in most of 13 Amazonian fishes exposed to > 33°C over 10 to 30 days (*28*). The direct effects of warm temperature on fish can be exacerbated by the reduction in dissolved oxygen in warm waters[40], as hypoxia tolerance is reduced in Amazonian fishes after short and long-term exposure to > 33°C (*28*). The heatwave during the 2023 drought also impacted aquaculture of tropical fish, with one instance where 3,000 fish died in one aquaculture pond (*29*). Indeed, warming in the near future may impair the farming of *Colossoma macropomum* that is responsible for a large fraction of Amazonian aquaculture production (*30*, *31*).

Existing compilations of global lake water temperature seldom include in situ data for Amazonian lakes, and tropical systems are underrepresented in global networks of lake observations (*32*, *33*), even though recent global studies based on satellite data did include tropical lakes (*34*–*36*). The development of consistent, long-term environmental monitoring of vulnerable lake ecosystems such as Tefé and Coari lakes is imperative for them to be effective sentinels of climate change and to develop management strategies of value to the inhabitants of the region. Such long-term monitoring will enable us to assess the vulnerability of Amazonian water bodies – and other freshwaters across the tropics – to climate change, including the associated warming and alterations to the hydrological cycle that lead to extreme drought and heatwaves. Climate models project increasing air temperatures across the globe, yet the impact of climate change on tropical waters remains largely unknown. A better understanding of how freshwater biodiversity and the provision of ecosystem services may change in a warming world is essential to inform science-based actions to protect and adaptively manage these vulnerable ecosystems.

References and Notes

1. C. M. O'Reilly, S. Sharma, D. K. Gray, S. E. Hampton, J. S. Read, R. J. Rowley, P. Schneider, J. D. Lenters, P. B. McIntyre, B. M. Kraemer, G. A. Weyhenmeyer, D. Straile, B. Dong, R. Adrian, M. G. Allan, O. Anneville, L. Arvola, J. Austin, J. L. Bailey, J. S. Baron, J. D. Brookes, E. de Eyto, M. T. Dokulil, D. P. Hamilton, K. Havens, A. L. Hetherington, S. N. Higgins, S. Hook, L. R. Izmest'eva, K. D. Joehnk, K. Kangur, P. Kasprzak, M. Kumagai, E. Kuusisto, G. Leshkevich, D. M. Livingstone, S. MacIntyre, L. May, J. M. Melack, D. C. Mueller-Navarra, M. Naumenko, P. Noges, T. Noges, R. P. North, P. Plisnier, A. Rigosi, A. Rimmer, M. Rogora, L. G. Rudstam, J. A. Rusak, N. Salmaso, N. R. Samal, D. E. Schindler, S. G. Schladow, M. Schmid, S. R. Schmidt, E. Silow, M. E. Soylu, K. Teubner, P. Verburg, A. Voutilainen, A. Watkinson, C. E. Williamson, G. Zhang, Rapid and highly variable warming of lake surface waters around the globe. *Geophys. Res. Lett.* **42**, 1–9 (2015).
2. M. T. Dokulil, E. de Eyto, S. C. Maberly, L. May, G. A. Weyhenmeyer, R. I. Woolway, Increasing maximum lake surface temperature under climate change. *Clim. Change*. **165**, 56 (2021).
3. R. I. Woolway, C. Albergel, T. L. Frölicher, M. Perroud, Severe Lake Heatwaves Attributable to Human-Induced Global Warming. *Geophys. Res. Lett.* **49**, 1–10 (2022).
4. X. Wang, K. Shi, Y. Zhang, B. Qin, Y. Zhang, W. Wang, R. I. Woolway, S. Piao, E. Jeppesen, Climate change drives rapid warming and increasing heatwaves of lakes. *Sci. Bull.* **68**, 1574–1584 (2023).
5. C. E. Williamson, J. E. Saros, W. F. Vincent, J. P. Smol, Lakes and reservoirs as sentinels, integrators, and regulators of climate change. *Limnol. Oceanogr.* **54**, 2273–2282 (2009).
6. S. K. Hamilton, Biogeochemical implications of climate change for tropical rivers and floodplains. *Hydrobiologia*. **657**, 19–35 (2010).
7. J. Talling, John; Lemoalle, *Ecological dynamics of tropical inland waters* (Cambridge University Press, ed. 1, 1998).
8. S. MacIntyre, J. R. Romero, G. W. Kling, Spatial-temporal variability in surface layer deepening and lateral advection in an embayment of Lake Victoria, East Africa. *Limnol. Oceanogr.* **47**, 656–671 (2002).
9. S. Macintyre, J. R. Romero, G. M. Silsbe, B. M. Emery, Stratification and horizontal exchange in lake victoria, East africa. *Limnol. Oceanogr.* **59**, 1805–1838 (2014).
10. Z. Xing, D. A. Fong, E. Y. M. Lo, S. G. Monismith, Thermal structure and variability of a shallow tropical reservoir. *Limnol. Oceanogr.* **59**, 115–128 (2014).
11. W. Zhou, J. M. Melack, S. MacIntyre, P. M. Barbosa, J. H. F. Amaral, A. Cortés, Hydrodynamic Modeling of Stratification and Mixing in a Shallow, Tropical Floodplain Lake. *Water Resour. Res.* **60**, 1–21 (2024).
12. S. Perkins-Kirkpatrick, D. Barriopedro, R. Jha, L. Wang, A. Mondal, R. Libonati, K. Kornhuber, Extreme terrestrial heat in 2023. *Nat. Rev. Earth Environ.* **5**, 2023–2025 (2024).
13. J. C. Espinoza, J. C. Jimenez, J. A. Marengo, J. Schongart, J. Ronchail, W. Lavado-Casimiro, J. V. M. Ribeiro, The new record of drought and warmth in the Amazon in 2023

related to regional and global climatic features. *Sci. Rep.* **14**, 8107 (2024).

14. M. Rantanen, A. Laaksonen, The jump in global temperatures in September 2023 is extremely unlikely due to internal climate variability alone. *npj Clim. Atmos. Sci.* **7**, 34 (2024).

15. G. Schmidt, Climate models can't explain 2023's huge heat anomaly — we could be in uncharted territory. *Nature*. **627**, 467–467 (2024).

16. F. Costa, J. Marengo, "Statement on the 2023 Amazon drought and its unforseen consequences" (2023), (available at https://www.theamazonwewant.org/spa-reports/).

17. M. Marmontel, A. Fleischmann, A. Val, B. Forsberg, Safeguard Amazon's aquatic fauna against climate change. *Nature*. **625**, 450–450 (2024).

18. E. M. Latrubesse, "Amazon lakes" in *Encyclopedia of Earth Sciences Series* (2012).

19. G. Irion, J. A. S. N. De Mello, J. Morais, M. T. F. Piedade, W. J. Junk, L. Garming, "Development of the Amazon Valley During the Middle to Late Quaternary : Sedimentological and Climatological Observations" in *Amazonian Floodplain Forests*, W. Junk, M. Piedade, F. Wittmann, J. Schöngart, P. Parolin, Eds. (Springer Science+Business Media B.V. 2010, 2010).

20. S. C. Maberly, R. A. O'Donnell, R. I. Woolway, M. E. J. Cutler, M. Gong, I. D. Jones, C. J. Merchant, C. A. Miller, E. Politi, E. M. Scott, S. J. Thackeray, A. N. Tyler, Global lake thermal regions shift under climate change. *Nat. Commun.* **11**, 1232 (2020).

21. D. F. Campos, A. L. Val, V. M. F. Almeida-Val, The influence of lifestyle and swimming behavior on metabolic rate and thermal tolerance of twelve Amazon forest stream fish species. *J. Therm. Biol.* **72**, 148–154 (2018).

22. A. L. Val, M. e. N. Paula-Silva, V. M. F. Almeida-Val, C. M. Wood, In vitro effects of increased temperature and decreased pH on blood oxygen affinity of 10 fish species of the Amazon. *J. Fish Biol.* **89**, 264–279 (2016).

23. R. I. Woolway, I. D. Jones, S. C. Maberly, J. R. French, D. M. Livingstone, D. T. Monteith, G. L. Simpson, S. J. Thackeray, M. R. Andersen, R. W. Battarbee, C. L. DeGasperi, C. D. Evans, E. de Eyto, H. Feuchtmayr, D. P. Hamilton, M. Kernan, J. Krokowski, A. Rimmer, K. C. Rose, J. A. Rusak, D. B. Ryves, D. R. Scott, E. M. Shilland, R. L. Smyth, P. A. Staehr, R. Thomas, S. Waldron, G. A. Weyhenmeyer, Diel Surface Temperature Range Scales with Lake Size. *PLoS One*. **11**, e0152466 (2016).

24. J. Du, P. A. Jacinthe, H. Zhou, X. Xiang, B. Zhao, M. Wang, K. Song, Monitoring of water surface temperature of Eurasian large lakes using MODIS land surface temperature product. *Hydrol. Process.* **34**, 3582–3595 (2020).

25. R. I. Woolway, B. M. Kraemer, J. D. Lenters, C. J. Merchant, C. M. O'Reilly, S. Sharma, Global lake responses to climate change. *Nat. Rev. Earth Environ.* **1**, 388–403 (2020).

26. T. P. Hughes, J. T. Kerry, A. H. Baird, S. R. Connolly, A. Dietzel, C. M. Eakin, S. F. Heron, A. S. Hoey, M. O. Hoogenboom, G. Liu, M. J. McWilliam, R. J. Pears, M. S. Pratchett, W. J. Skirving, J. S. Stella, G. Torda, Global warming transforms coral reef assemblages. *Nature*. **556**, 492–496 (2018).

27. E. J. Walter, M. Carraretto, The neurological and cognitive consequences of hyperthermia.

Crit. Care. **20**, 199 (2016).

28. E. H. Jung, K. V. Brix, J. G. Richards, A. L. Val, C. J. Brauner, Reduced hypoxia tolerance and survival at elevated temperatures may limit the ability of Amazonian fishes to survive in a warming world. *Sci. Total Environ.* **748**, 141349 (2020).

29. V. Souza, "Cozinhou a plantação": seca no Norte leva a perda de lavouras, e calor mata milhares de peixes (2023), (available at https://g1.globo.com/economia/agronegocios/noticia/2023/10/20/cozinhou-a-plantacao-seca-no-norte-leva-a-perda-de-lavouras-e-calor-mata-milhares-de-peixes.ghtml).

30. J. C. da Costa, A. L. Val, Extreme climate scenario and parasitism affect the Amazonian fish Colossoma macropomum. *Sci. Total Environ.* **726**, 138628 (2020).

31. L. A. L. Pereira, R. D. Amanajás, A. M. de Oliveira, M. de N. Paula da Silva, A. L. Val, Health of the Amazonian fish tambaqui (Colossoma macropomum): Effects of prolonged photoperiod and high temperature. *Aquaculture*. **541** (2021), doi:10.1016/j.aquaculture.2021.736836.

32. S. Sharma, D. K. Gray, J. S. Read, C. M. O'Reilly, P. Schneider, A. Qudrat, C. Gries, S. Stefanoff, S. E. Hampton, S. Hook, J. D. Lenters, D. M. Livingstone, P. B. McIntyre, R. Adrian, M. G. Allan, O. Anneville, L. Arvola, J. Austin, J. Bailey, J. S. Baron, J. Brookes, Y. Chen, R. Daly, M. Dokulil, B. Dong, K. Ewing, E. de Eyto, D. Hamilton, K. Havens, S. Haydon, H. Hetzenauer, J. Heneberry, A. L. Hetherington, S. N. Higgins, E. Hixson, L. R. Izmest'eva, B. M. Jones, K. Kangur, P. Kasprzak, O. Köster, B. M. Kraemer, M. Kumagai, E. Kuusisto, G. Leshkevich, L. May, S. MacIntyre, D. Müller-Navarra, M. Naumenko, P. Noges, T. Noges, P. Niederhauser, R. P. North, A. M. Paterson, P.-D. Plisnier, A. Rigosi, A. Rimmer, M. Rogora, L. Rudstam, J. A. Rusak, N. Salmaso, N. R. Samal, D. E. Schindler, G. Schladow, S. R. Schmidt, T. Schultz, E. A. Silow, D. Straile, K. Teubner, P. Verburg, A. Voutilainen, A. Watkinson, G. A. Weyhenmeyer, C. E. Williamson, K. H. Woo, A global database of lake surface temperatures collected by in situ and satellite methods from 1985–2009. *Sci. Data*. **2**, 150008 (2015).

33. D. Naderian, R. Noori, E. Heggy, S. M. Bateni, R. Bhattarai, A. Nohegar, S. Sharma, A water quality database for global lakes. *Resour. Conserv. Recycl.* **202**, 107401 (2024).

34. Y. Tong, L. Feng, X. Wang, X. Pi, W. Xu, R. I. Woolway, Global lakes are warming slower than surface air temperature due to accelerated evaporation. *Nat. Water*. **1**, 929–940 (2023).

35. F. Yao, B. Livneh, B. Rajagopalan, J. Wang, J. Crétaux, Satellites reveal widespread decline in global lake water storage. **749**, 743–749 (2023).

36. R. I. Woolway, Y. Tong, L. Feng, G. Zhao, D. A. Dinh, H. Shi, Y. Zhang, K. Shi, Multivariate extremes in lakes. *Nat. Commun.* **15**, 4559 (2024).

Acknowledgments: We thank Cristiane K. M. Kolesnikovas from Associação R3 Animal for discussing the results. We thank WWF-Brasil for providing the water temperature sensors used during the dolphin Unusual Mortality Event, and Cláudio Barbosa (INPE) that provided the

ADCP equipment. We are also grateful to the Google Earth Engine team for the support for data processing.

Funding: Provide complete funding information, including grant numbers, complete funding agency names, and recipient's initials. Each funding source should be listed in a separate paragraph.

Fundação de Amparo à Pesquisa do Estado do Amazonas (FAPEAM), Secretaria de Estado de Desenvolvimento Econômico, Ciência, Tecnologia e Inovação (SEDECTI) and the Governo do Estado do Amazonas grant EDITAL N.º 006/2022 (Project "Mudanças climáticas e recursos hídricos nas várzeas do Solimões") (ASF)

Gordon and Betty Moore Foundation, grant "Advancing the understanding of methane emissions from tropical wetlands"

National Science Foundation, grant "CNH2-L project"

CNPq, grant PCI Program (PA, AZ)

French National Research Institute for Sustainable Development, grant JEAI/AMAWE

CNES, grant "SWOT for SOUTH AMERICA" and "SAMBA" (FP, ASF, DM)

US National Science Foundation (Division of Environmental Biology), grant number 1753856 (JM, WZ, SM).

Author contributions: Each author's contribution(s) to the paper should be listed [we encourage you to follow the CRediT model]. Each CRediT role should have its own line, and there should not be any punctuation in the initials.

Conceptualization: ASF, FP, SH, JM, BF, WC, LL, JR, BA, MM

Data curation: ASF, LL, JR, BA, BM, PA, MB, LC, MG, DH, IK, RM, RN, PS, CV, RX, AZ, WZ, SM, NF, RM, ES, WG, AC, HP, SM, MN, DM, LS, JP, MM

Investigation: ASF, FP, SH, JM, BF, AV, WC, LL, JR, BA, BM, PA, MB, LC, MG, DH, IK, RM, RN, PS, CV, RX, AZ, AR, WZ, SM, EM, NF, RM, ES, MF, RO, LL, WG, AC, HP, SM, MN, DM, LS, JP, MM

Methodology: ASF, FP, SH, JM, BF, WC, LL, JR, BA, AR, DM, MM

Project administration: ASF, MM

Writing – original draft: ASF, FP, SH, JM, AV, BF, LL, JR, EM, MM

Writing – review & editing: ASF, FP, SH, JM, BF, AV, WC, LL, JR, BA, BM, PA, MB, LC, MG, DH, IK, RM, RN, PS, CV, RX, AZ, AR, WZ, SM, EM, NF, RM, ES, MF, RO, LL, SM, MN, DM, MM

Competing interests: Authors declare that they have no competing interests.

Data and materials availability: All in situ data (water temperature) used in this article will be deposited into Zenodo platform before final publication. Remote sensing data can be assessed in the GitHub link: < https://github.com/leolaipelt/water_surface_temperature>.

Codes used for remote sensing data processing are available at: < https://github.com/leolaipelt/water_surface_temperature>.

Supplementary Materials

Materials and Methods
Supplementary Text 1
Figs. S1 to S10

Materials and Methods

Field data collection. Water temperatures were measured in several Amazonian lakes during the 2023 drought. In Tefé Lake, six Hobo Pendant MX2201 water temperature loggers were suspended on a line at different depths depending on total water depths (including 0.3 and 2 m, if possible, see locations in Figure 1e). From Sep 28 to Nov 9, water temperature, conductivity and pH were measured daily around 16h local time with a Hannah HI 98194 multiparameter probe at the surface, 50% of the water column depth, and near the bottom. Secchi disk depth (19 cm diameter) was measured at the same sites. At site 4 (Figure 1e), a pressure transducer (Solinst Levelogger 5) was installed at the bottom to measure water depth and water temperature; water level measurements were compensated for atmospheric pressure with a Solinst Barologger 5) installed at the same site.

Temperature loggers were installed in nine other lakes across the central Amazon (Table 1): three floodplain lakes in the Mamirauá Sustainable Development Reserve (Samaumeirinha, Cedrinho and Buá-Buá); Amanã Lake, a ria lake to the north of Tefé in the Amanã Sustainable Development Reserve; Coari Lake, a ria lake around 200 km downstream from Tefé along the Amazon River which also faced dolphin mortality; and four other floodplain lakes near Manaus (Janauacá, Miriti, Calado and Castanho). Hobo Pendant MX2201 sensors have an estimated accuracy of ±0.5°C, Solinst Levelogger of ±0.05°C, RBRsolo of ±0.002°C, and Hannah probe of ±0.15°C – the locations where they were deployed are presented in Table 1.

A long-term environmental monitoring program (since 2004) at Tefé Lake has been conducted by the Mamirauá Institute, sampling monthly downstream 1 km from the urban area of Tefé. A Hannah HI 98194 multiparameter probe was normally used to take measurements at 0.1, 0.5, 1.0, 2.0 and 3.5 m depths).

Longitudinal profiles of near-surface water temperatures in the Tefé Lake channel were acquired with a hull-mounted Garmin Echosounder Echomap Plus 42 cv, which includes a temperature sensor. The same equipment was used to map Tefé Lake's bathymetry in the downstream portion of the lake, covering an area of around 30 km², as depicted in Figure 1d. Water velocities and discharge in the Tefé Lake channel were measured at locations 1, 3 and 4 (see map in Figure 1e) with an acoustic Doppler current profiler (SonTek RiverCat). In the lower Amazon, two campaigns (in 2021 and 2023; Figure S8) were conducted to estimate longitudinal profiles of near-surface water temperature using the Garmin Echosounder Echomap Plus 62 cv.

Table 1. Locations and other information about *in situ* measurements of water temperatures.

Lake name	Coordinates (Lat/Lon)	Gauge number	Sampling rate	Data collection period	Depth of measurement (m)	Lake depth at the site during the 2023 drought (m)	Sensor type
Tefé	-3.341620, -64.7304019	1	1 min	03/10/2023 – 25/11/2023	0.3	0.8	HOBO Pendant MX2201 Temperature
	-3.334398, -64.72372	2	1 min	18/10/2023 - 31/10/2023	0.3	1.2	HOBO Pendant MX2201 Temperature
	-3.338512, -64.7167479	3	1 min	03/10/2023 – 03/11/2023	0.3	2.5	HOBO Pendant MX2201 Temperature
	-64.703285, -3.335440	4	10 min	01/10/2023 - 04/06/2024	0.3	5.0	Solinst levelogger 5
	-64.703285, -3.335440	4	10 min	11/10/2023 - 04/06/2024	Bottom	5.0	
	-3.3338320, -64.6978129	5	1 min	11/10/2023 – 11/12/2023	0.3	4.0	HOBO Pendant MX2201 Temperature
	-3.3338320, -64.6978129	5	1 min	03/11/2023 - 11/12/2023	2	4.0	
	-3.3531440, -64.6772239	6	1 min	03/10/2023 - 04/06/2024	0.3	3.0	HOBO Pendant MX2201 Temperature
Coari	-4.029051, -63.22943	1	10 min	03/11/2023 - 28/11/2023	0.3	0.5	HOBO Pendant MX2201 Temperature

Coari	-4.08089, -63.150354	2	10 min	03/11/2023 - 28/11/2023	0.3	1.0	HOBO Pendant MX2201 Temperature
Cedrinho	-2.804494, -65.089030	-	1 hour	10/03/2023 - 23/01/2024	Lake bottom	1.3	Solinst levelogger 5
Buá-Buá	-2.893348, -64.978020	-	1 hour	20/01/2023 - 12/01/2024	Lake bottom	1.0	Solinst levelogger 5
Samaumeirinha	-2.81686, -65.03215	-	5 min	31/10/2023 – 13/12/2023	Lake bottom	1.0	HOBO Pendant MX2201 Temperature
Amanã	-2.68111, -64.620414	-	10 min	17/10/2023 –	0.3 and 2.0	5.0	HOBO Pendant MX2201 Temperature
Janauacá	-3.384027778, -60.22938889 -3.409694444, -60.26227778 -3.399472222, -60.27716667 -3.387611111, -60.29536111 -3.414138889, -60.24991667	-	One date of sampling only; five locations of measurements	10/10/2023	0 (surface)	0.2 – 0.6	YSI Professional Plus Multiparameter Probe

	-3.387888889, -60.23941667						
Calado	-3.2779364, -60.58000077	-	15 min	23/11/2023-18/12/2023	0 (surface)	0.5	RBRsolo
Miriti	-3.2626915, -60.9278346	-	15 min	23/11/2023-18/12/2023	0 (surface)	4.5	RBRsolo
Castanho	-3.8260412, -60.3651480	-	15 min	22/11/2023-19/12/2023	0 (surface)	4.8	RBRsolo

Climate data. Meteorological data were obtained from reanalysis datasets from ECMWF and ERA-Land for surface air temperature, relative humidity, and rainfall using the Google Earth Engine platform (Gorelick et al., 2017). *In situ* weather data (rainfall rates, sunlight hours, wind speed and air temperature) were obtained from the Brazilian National Institute of Meteorology (available at: <https://portal.inmet.gov.br/>) for the following central Amazon stations: Benjamin Constant (INMET code 82410); Tefé (82317) and Manaus (82331). For the Tefé Lake analysis, *in situ* lake water level and rainfall data during the 2023 drought were obtained from the monitoring network maintained by the Mamirauá Institute, which includes a water level gauge (combined Solinst Levelogger 5 and manual rule, both georeferenced to EGM2008 datum) and a DualBase automatic tipping bucket rainfall gauge (https://www.dualbase.com.br/produtos/sensores/precipitacao-pluviometrica).

Surface water extent. The surface water extent was calculated for each lake using multispectral data from Landsat Collection 2. Data were acquired using the Google Earth Engine cloud computing platform for the Landsat 5 Thematic Mapper (TM), Landsat 7 Enhanced Thematic Mapper Plus (ETM+), Landsat 8 Operational Land Imager (OLI) and Thermal Infrared Sensor (OLI/TIRS), and Landsat 9 OLI-2 and TIRS-2. The Landsat data are available at https://developers.google.com/earth-engine/datasets/catalog/landsat. We used the Normalized Difference Water Index (NDWI) to estimate the water mask for each Landsat scene, considering only pixels greater than zero as water surface, using Eq. 1.

$$NDWI = \frac{\rho_{green} - \rho_{swir1}}{\rho_{green} + \rho_{swir1}} \quad (1)$$

where ρ_{green} and ρ_{swir1} are the green (0.52–0.60 and 0.53–0.59 μm ranges, respectively, for Landsat 5/7 and 8/9) and shortwave infrared bands (1.55–1.75 and 1.57–1.65 μm ranges, respectively, for Landsat 5/7 and 8/9).

Satellite water surface temperature. Landsat images were used to obtain water surface temperature (WST) anomalies for Amazonian lakes at 30 m spatial resolution. Data from Landsat 5, 7, 8 and 9 from the Landsat Collection 2 were acquired using the Google Earth Engine (available at https://developers.google.com/earth-engine/datasets/catalog/landsat). Landsat Collection 2 images are provided with an atmospheric correction: USGS Land Surface Reflectance Code (LaSRC) version 1.5.0 (derived from NASA LaSRC version 3.5.5), for OLI/TIRS, and USGS Landsat Ecosystem Disturbance Adaptive Processing System (LEDAPS) Surface Reflectance algorithm version 3.4.0 (derived from the February 2011 version of NASA LEDAPS code) for For TM and ETM+.

Pixel quality attributes were used to filter cloud cover and presence of water (based on NDWI, see Equation 1). WST was estimated with Landsat images according to Equation 2[33]:

$$WST = \frac{K_2}{\ln\left[\left(\frac{\varepsilon_{nb} K_1}{R_c}\right)+1\right]} \quad (2)$$

where ε_{nb} is the narrow band emissivity obtained from NDVI[34]. The K_1 and K_2 are constants obtained from image properties for each Landsat product (K_1 is equal to 607.76, 666.09, 774.8853 and 774.8853 $W \cdot m^{-2} \cdot sr^{-1} \cdot \mu m^{-1}$ and K_2 is equal to 1260.56, 1282.71, 1321.0789 and 1321.0789 $W \cdot m^{-2} \cdot sr^{-1} \cdot \mu m^{-1}$, respectively, for Landsat 5, 7, 8 and 9). R_c is the corrected thermal radiance from the surface ($W \cdot m^{-2} \cdot sr^{-1} \cdot \mu m^{-1}$), computed according to Equation 3[33,35]:

$$R_c = \frac{R_{TOA} - R_p}{\tau_{NB}} - (1 - \varepsilon_{NB}) R_{sky} \quad (3)$$

where R_{TOA} is the thermal radiation at the top of atmosphere ($W \cdot m^{-2} \cdot sr^{-1} \cdot \mu m^{-1}$), which was obtained by the brightness temperature from Landsat data. R_p is the path radiance (0.91 $W \cdot m^{-2} \cdot sr^{-1} \cdot \mu m^{-1}$), R_{sky} is the narrow band downward thermal radiation from a clear sky (1.32 $W \cdot m^{-2} \cdot sr^{-1} \cdot \mu m^{-1}$) and τ_{NB} is the narrow band transmissivity of air (0.866 μm)[33].

Regarding the accuracy for different Landsat missions, Barsi et al.[39] showed that Landsat 7 is calibrated for no residual gain or offset error for the lifetime to within ± 0.55 ºC and Landsat 5 is calibrated to within ± 0.67 ºC. Moreover, Vanhellemont[40] evaluated the performance of the Landsat 8 WST in cloud-free conditions with in situ measurements and founded an RMSD of 0.7–1 ºC and low bias of <0.3 ºC. Considering the comparison of different thermal sensors and algorithms, Meng et al.[41] showed that the Landsat 9 LST presented absolute differences from MODIS LST (MOD11 and MOD21) in a range of 0.01 to 2.50 ºC. Hulley et al.[42] found that the LST from the Moderate Resolution Imaging Spectroradiometer (MODIS) MYD21 LST and the Visible Infrared Imager Radiometer Suite (VIIRS) VNP21 have a small bias of less than 0.5 ºC.

Landsat data have been used to investigate lake WST patterns in several studies[36–38]. Sharma et al.[31] compared global estimates of satellite-derived WST using the Advanced Very High Resolution Radiometer (AVHRR) and the Along Track Scanning Radiometer (ATSR) imagery with in situ observations and found an RMSE of 1.15 °C for summertime mean values and a RMSE of 0.72 °C for interannual anomalies.

Here, the results for central Amazon lakes are assessed as anomalies, which reduces error due to bias. A total of 24 lakes were selected in the central Amazon, and are representative of the region's largest water bodies. The Landsat thermal infrared datasets have special resolution of 120, 60 and 100 m for Landsat 5 TM, Landsat 7 ETM+, Landsat 8 TIRS/Landsat 9 TIRS-2, respectively. The images were resampled to 30 m with a cubic convolution method. Only pixels with water were selected using a mask based on NDWI (i.e., NDWI > 0); the criterium was successfully validated with visual inspection with visible satellite observations of the lakes' dry areas.

WST is measured in the field usually at depths of a few centimeters below the surface[43]. This differs from satellite-derived WST, also called radiometric skin temperature, which represents an extremely thin layer of the water surface (less than 1 mm thick)[44]. The skin and sub-skin lake surface temperature often differs in the order of 0.2 °C, varying due to meteorological conditions (e.g. wind speed)[43]. Landsat data acquisitions in the analyzed Amazonian lakes occur in mid-morning (equatorial crossing at about 9:30 am local time). Thus, the skin temperatures reflected morning conditions.

Landsat scenes with cloud cover (Landsat filter) higher than 20% were disregarded. Hence, most of the available images are representative of the period from June to Oct (dry season). The number of Landsat scenes used per year were, on average and considering all lakes, 85 for the period from 1990 to 1998 (only Landsat 5), 132 from 1999 to 2020 (both Landsat 7 and 8) and 185 after 2021 (with both Landsat 8 and 9). Moreover, WST was limited to a range between 15–45°C to avoid erroneous under- and overestimation. Trend analysis using monthly average water temperature revealed anomalies based on the mean for each month over the entire period of analysis (1990–2023). Increasing or decreasing trends were evaluated using the Mann-Kendall Test.

Numerical modeling of extreme water temperatures. To demonstrate that changes in ambient meteorology and decreases in the transparency of the lake water could lead to the extreme temperatures observed in Tefé Lake in Oct

2023, we used the 3-Dimensional coupled Hydrodynamic-Aquatic Ecosystem Model (AEM3D) developed to model stratification and mixing in a similar lake on the Amazon floodplain. Prior to these simulations, Zhou et al. (2024) rigorously evaluated AEM3D's ability to simulate temperature and density structure over diel periods in Janauacá Lake (3.38°S, 60.3°W) using field measurements of water-column temperatures and meteorological data spanning two hydrological years. Simulated patterns of diel stratification and mixing matched measurements well. The hydrodynamic module of AEM3D uses a z-coordinate Cartesian grid allowing non-uniform spacing in three directions and solves the unsteady Reynolds-averaged Navier-Stokes equations for momentum under the Boussinesq approximation, the continuity equations for incompressible fluids, and the transport equation for scalars. AEM3D was configured with a domain of 100 × 100 m mesh grids in the horizontal and 0.1 m layers in the vertical, and a time step of 30 s.

Meteorological measurements (wind speed and direction, air temperature, relative humidity) were made with sensors deployed on a floating platform in Janauacá Lake. Incoming shortwave and longwave radiation were measured in the open about 1 km from the region where simulations were conducted. The diffuse attenuation coefficient (k_d) of photosynthetically available radiation (PAR, 400 to 700 nm) was based on underwater PAR measurements in the lake; the highest value of 8.2 m^{-1} occurred when the water level was shallowest. Model details are fully explained in Zhou et al. (2024).

To understand the main factors that explain the observed heating of the floodplain lakes in 2023, we conducted a series of simulations for Janauacá Lake using various combinations and modifications of environmental conditions that were reasonable with respect to conditions in Oct 2023 in the central Amazon. AEM3D simulations were initialized with a temperature profile measured at Janauacá Lake when the water column was well mixed as water temperature varied by less than 0.02°C from surface to 6 m. The initial salinity profile was set to 0.0472 psu from surface to bottom based on CTD data measured at the lake. We made comparisons for clear and cloudy skies, air temperatures which were similar to measurements (x1) and 20% higher (x1.2); wind speed equivalent to measurements (x1) and 60% and 30% of measurements (x0.6, x0.3); a range of k_d (2.5, 6, 10 m^{-1}); and with water depths from 1 to 4 m.

Supplementary Text 1

Simulation of exceptional water temperatures in a central Amazon lake

To demonstrate that changes in ambient meteorology and decreases in the transparency of the lake water could lead to the extreme temperatures observed in Tefé Lake in Oct 2023, we used the 3-Dimensional coupled Hydrodynamic-Aquatic Ecosystem Model (AEM3D) developed to model stratification and mixing in a similar lake on the Amazon floodplain. The simulations showed that the exceptional water temperatures observed in Tefé Lake are expected when skies are clear, wind speeds are reduced, air temperatures are increased, and the turbidity of the water is high. Heat budgets for lakes include incoming and outgoing shortwave and longwave radiation, sensible heat flux (conduction), latent heat flux (evaporation), and advection. The clear skies and turbidity of the water led to increased absorption of solar radiation, the primary driver of the exceptionally high temperatures. Air temperatures were not a significant factor. The simulations also indicated that as water temperatures increased, greater heat losses via sensible heat exchange, latent heat exchange, and net longwave radiation occurred, as evidenced by the large diel variations in water temperature. The lower wind speeds were also a key contributor to warming by decreasing the sensible and latent heat fluxes, resulting in reduced heat losses from the water column.

Within three days of the start of simulations, water temperatures had increased to a maximum of 42.5^{o}C for the case of low wind speed, increased air temperature, increased k_d, and clear skies at the site (Fig. 2). The maximum temperature reached in the simulated domain was 42.8^{o}C (Fig. S10). As is typical for tropical lakes, the data illustrate a pattern of diurnal heating and nocturnal cooling with accompanying vertical mixing.

Fig. S1. Longitudinal profile of near-surface water temperatures along the Tefé Lake channel to its confluence with the Amazon River, as surveyed on Oct 2 afternoon. Background from Planet satellite imagery from Oct 18.

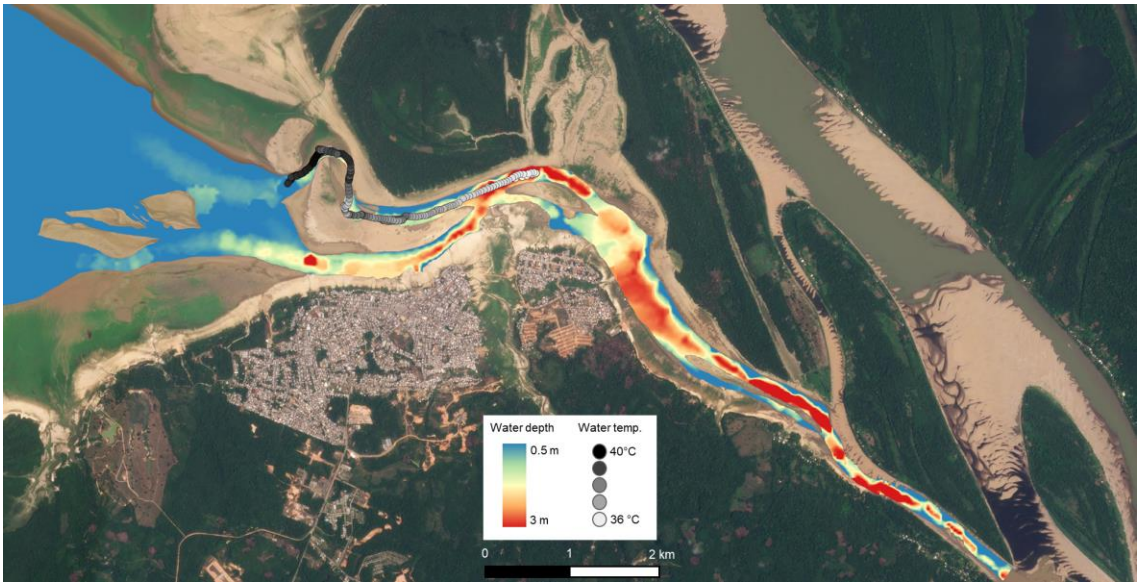

Fig. S2. Weather variables (solar radiation, air temperature, relative humidity, and wind speed) in the city of Tefé, derived from ERA5-Land hourly reanalysis data depict the 2023 drought. The top four charts show 2023 values compared to the minimum and maximum range (1954-2023). The driest and hottest day of 2023 was observed on Oct 9, when incoming radiation was also near the peak. The bottom four charts present the 2023 correspondent percentile for each day of the year (DOY). Solar radiation stayed above 70% between July and November, while wind speed was above the median (50%) for the same period. Extreme values were observed for air temperature and relative humidity during September and October 2023.

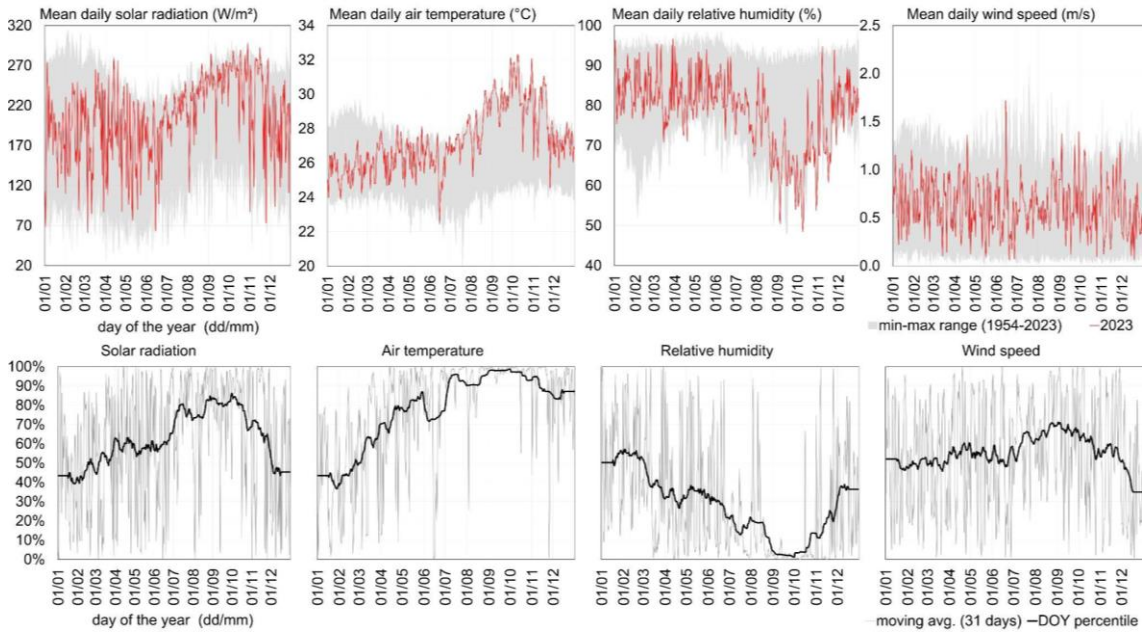

Fig. S3. The maximum sequence of clear-sky days in September-October in Tefé Lake based MODIS MYD09GA (bitmask algorithm).

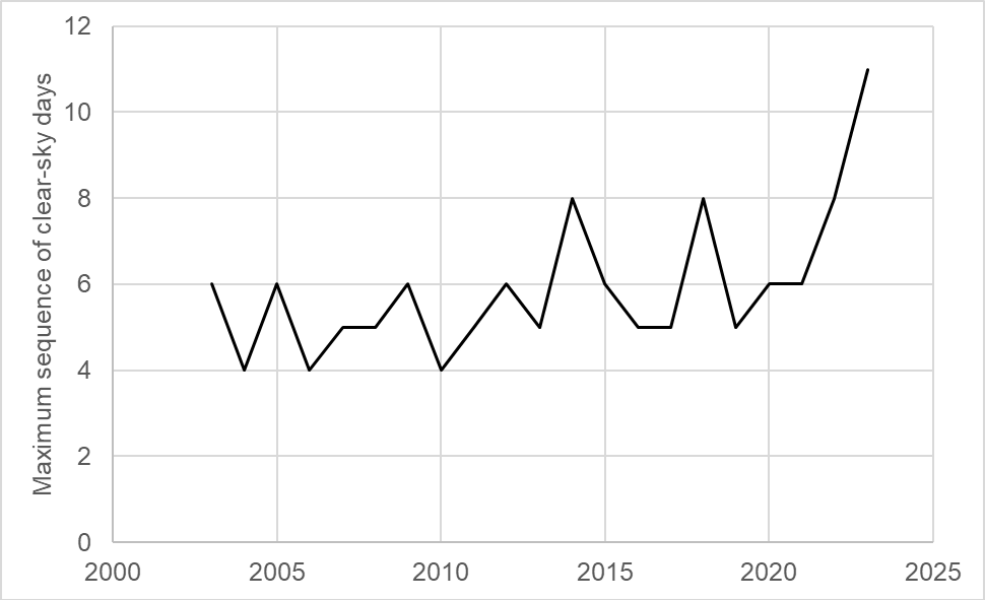

Fig. S4. Water quality parameters in Tefé Lake during the 2023 drought: water temperature and pH (measured with Hannah HI 98194 probes) and Secchi disk depth. All measurements are for the near surface; measurements from deeper depths were similar. Location of sites P1 to P4 is presented in the map.

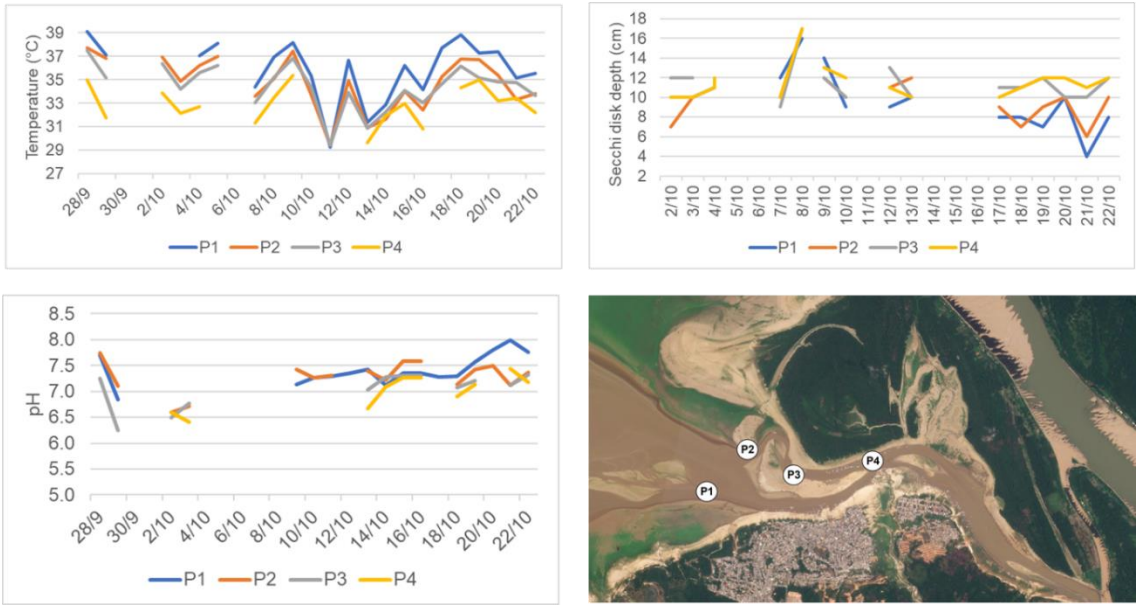

Fig. S5 (a) Water temperature at two different depths (0.3 m and 2 m) in Tefé Lake in 2023, showing the well-mixed water column during the drought, and larger differences between surface and 2-m deep waters after water levels started rising. (b) Consecutive days with high incoming solar radiation led to heat storage and progressively higher water temperatures.

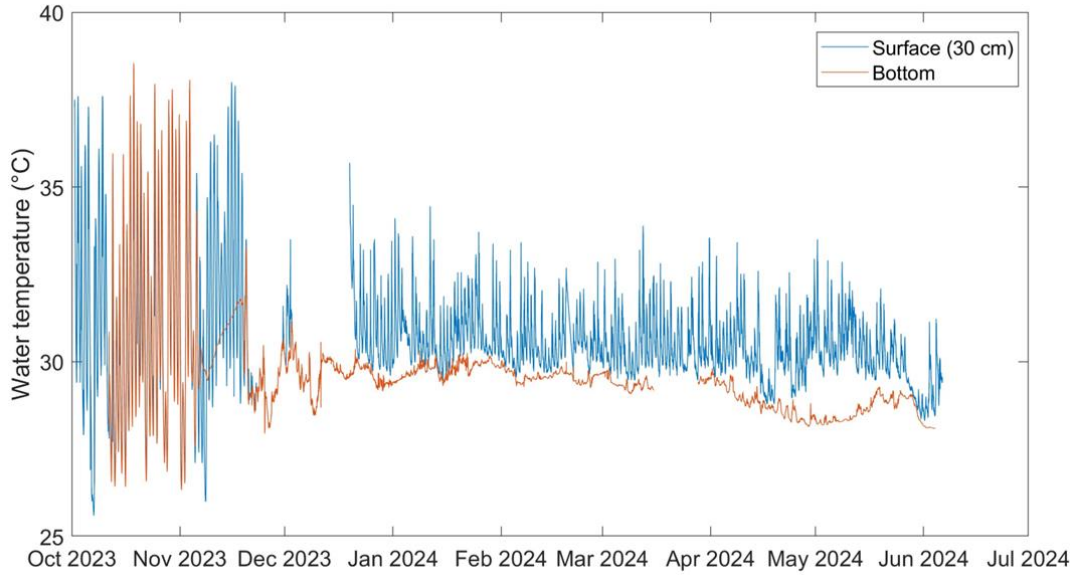

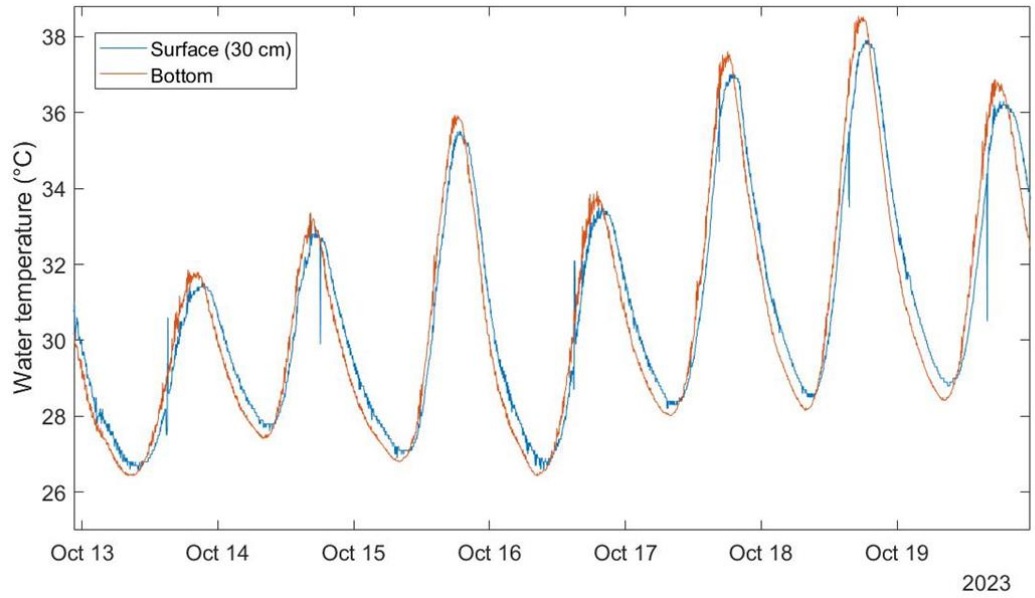

Fig. S6. Monthly surface air temperatures across the central Amazon from three in situ weather stations from Brazilian INMET.

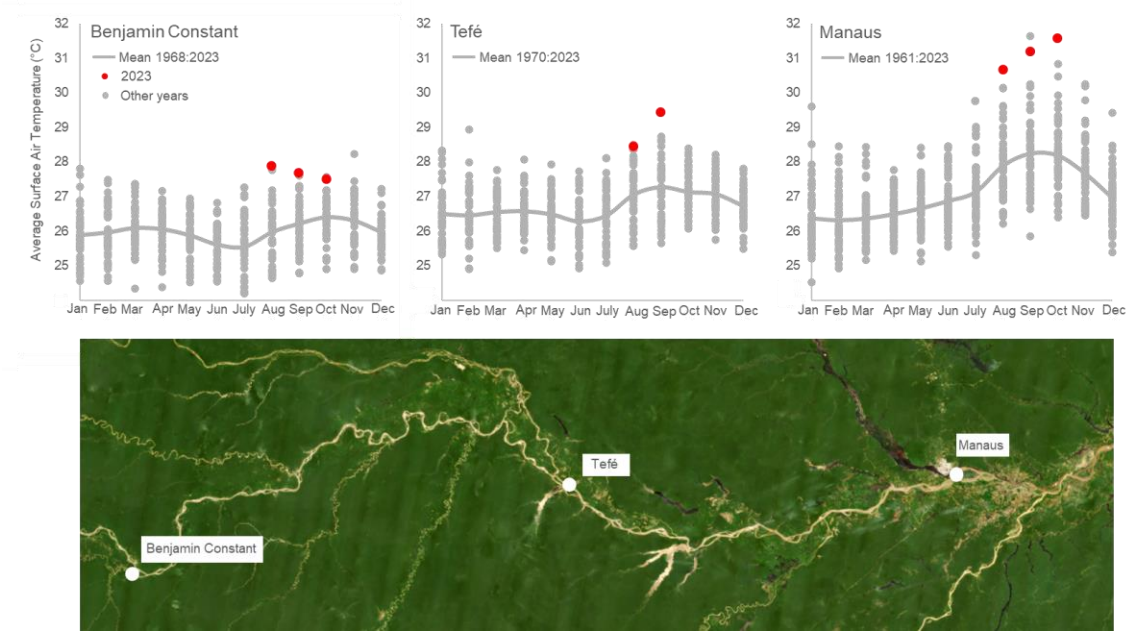

Fig. S7. Near-surface water temperatures along the Lower Amazon River for 2021 and 2023. Data presented only for afternoon hours.

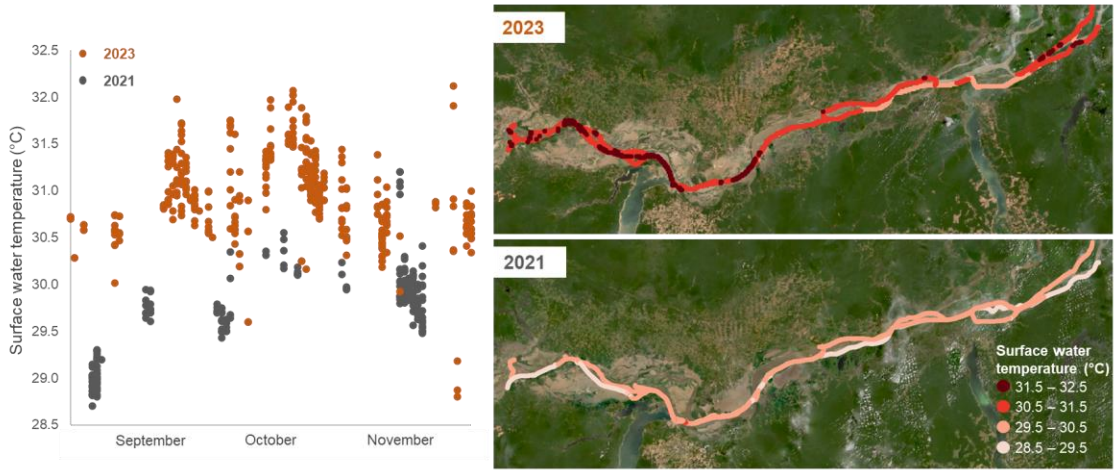

Fig. S8. Changes in water level and temperature in Coari Lake during the 2023 drought. Water temperatures were measured (10-min resolution) at the two sites depicted in the Fig.. Satellite image from Planet imagery shows the low Coari Lake on Oct 18, 2023.

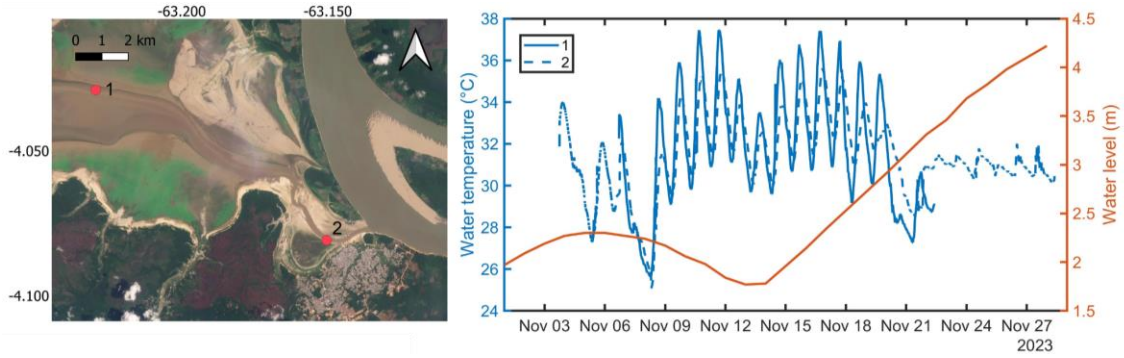

Fig. S9. Water temperature long-term trends (1990-2023) for each Amazonian lake analyzed in Fig 1. All lakes had significant positive trends at $p < 0.05$ (Mann-Kendall test). Long-term trend (°C per decade) is presented as a label for each lake.

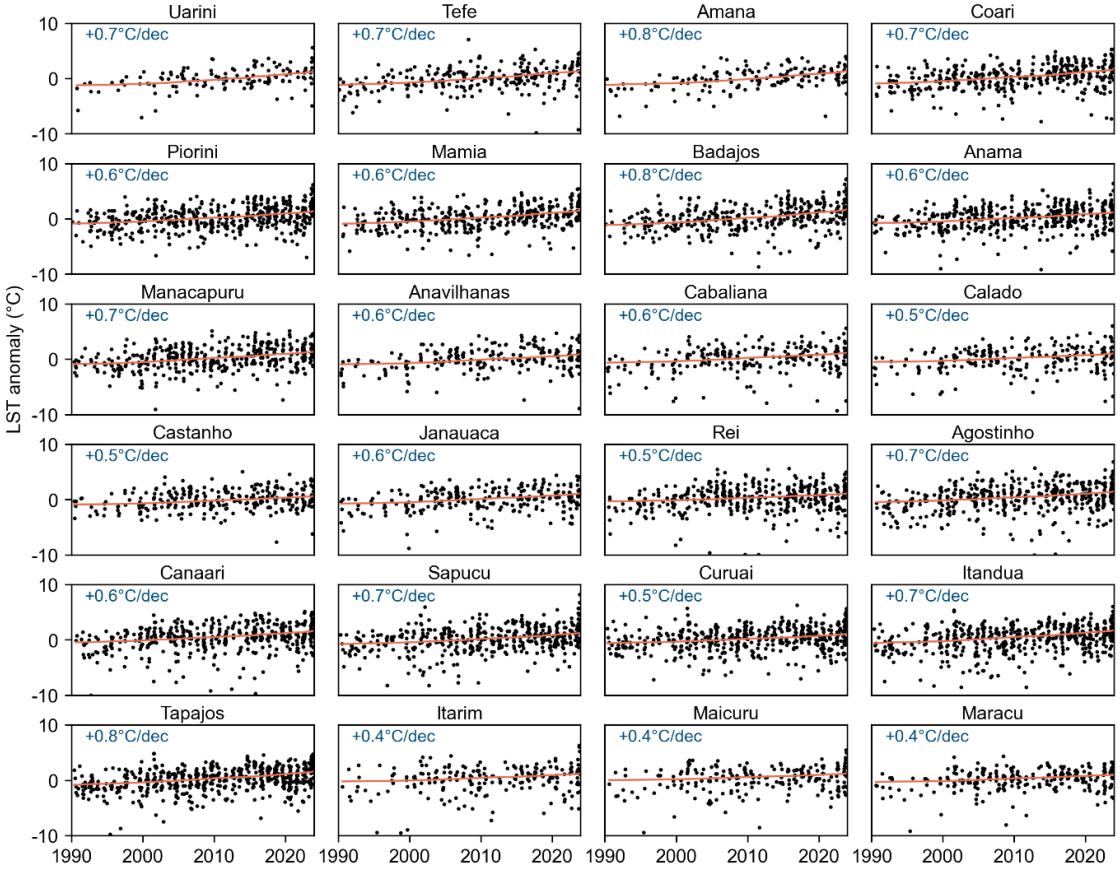

Fig. S10. A snapshot of simulated near-surface temperatures (day 3, 12:59). Wind speed and direction marked by the black arrow in lower left corner of the plot where blue and red circles mark wind speeds of 1.0 m s-1 and 2.0 m s-1, respectively.